(16) Fox, T. G. *Bull. Am. Phys. Soc.* **1952**, *2*, 493.
(17) Moskala, E. J.; Runt, J. P.; Coleman, M. M. Advances in Chemistry Series, No. 211, *Multicomponent Polymer Materials*, Paul, D. R., Sperling, L. H., Eds.; American Chemical Society: Washington, D. C.; Chapter 5, 1986.
(18) van Krevelen, P. W. *Properties of Polymers*; Elsevier: Amsterdam, 1972.
(19) Kraus, S. *J. Macromol. Sci., Rev. Macromol. Chem.* **1972**, *C7*-(2), 251.
(20) Hoy, K. L. *J. Paint Technol.* **1970**, *42*, 76.
(21) Fruitwala, H. M.S. Thesis, Imperial College, London, 1985.
(22) Neerinck, D.; van Audenhaege, A.; Lamberts, L. *Ann. Chim.* **1969**, *4*, 43.
(23) Sellier, G.; Wojtkowiak, B. *J. Chim. Phys. Physicochim. Biol.* **1968**, *65*(5), 936.
(24) Biros, J.; Zeman, L.; Patterson, D. *Macromolecules* **1971**, *4*, 30.
(25) Coleman, M. M.; Serman, C. J.; Painter, P. C. *Macromolecules* **1987**, *20*, 226.

High-Resolution Images of Defects in Liquid-Crystalline Polymers: Image Analysis Using Light Diffractometer and Computer Techniques

I. G. Voigt-Martin,* H. Durst, and H. Krug

Institut für Physikalische Chemie, Johannes Gutenberg Universität, Jakob-Welder Weg 15, D-6500 Mainz, West Germany. *Received May 3, 1988; Revised Manuscript Received August 8, 1988*

ABSTRACT: In an earlier paper, electron microscope images of smectic planes and lattice planes in liquid-crystalline polymers in smectic and crystalline phases were shown for the first time. Lattice defects in the form of edge dislocations were observed in both cases. The precise nature of the dislocation core and the planes in apparently disordered regions was not uniquely determined because of the poor signal/noise ratio. In this paper, two techniques of image reconstruction are demonstrated: light diffractometry and computer analysis. In both cases, considerably improved images are obtained. The analysis of defects is critically examined.

Introduction

Using high-resolution techniques, it has been possible to directly image the smectic planes in liquid-crystal (LC) polymers and the lattice planes in a crystalline LC polymer.[1-4] More important, it has been possible to demonstrate unambiguously the presence of edge dislocations in both systems.[5] At the same time, the structure of smectic planes in liquid crystals was shown to differ from lattice planes in crystalline LC polymers by the undulations which were always observed even in otherwise perfect regions. However, a few problems remain in the image analysis from the original micrographs, and they are inherent in the method of high-resolution imaging in low-contrast objects, namely the low signal/noise ratio. This problem becomes particularly aggravating in those regions where orientation is not perfect and in the regions close to the dislocation core.

There are two different approaches to this problem; both of them are very time consuming, but the improvement in image quality is very convincing. The first method involves the use of a light diffractometer and the second a computer. In this work, both techniques have been used, and the results are compared for identical locations on the specimen.

Image Reconstruction Using a Light Diffractometer

The method of image reconstruction using a light diffractometer is not new. It was used to obtain improved images of the tobacco mosaic virus in a classical paper by Klug and de Rosier[6] and is based on the methods discussed in books on optical transforms.[7] This technique, using a light diffractometer, involves two stages of transformation: the first from real space (the electron micrograph, which is the object) to reciprocal space (the Fourier transform of the electron micrograph) and back to real space (the Fourier transform of the intensity distribution in reciprocal space, which is the image). The diffraction pattern includes the Fourier frequencies from the desired structure, such as the smectic planes, as well as those from the background noise. By allowing only those spatial frequencies obtained from the smectic planes to pass through an aperture situated in the reciprocal plane, the noise can be filtered out of the micrograph. An example of such a procedure is shown in Figure 1. It is clear that the filtered image is a considerable improvement over the unfiltered one with regard to the signal/noise (S/N) ratio. However, with the aid of Figure 2, showing the diffraction pattern obtained by light diffractometry of the micrograph in Figure 1a, it is convenient to demonstrate some technical difficulties: The sharp maxima in the light diffractogram arise from the smectic planes, while the "amorphous" halo is produced by the noise in the electron micrograph. The radius of the halo depends on the precise value of defocus which was used in obtaining the original electron micrograph. This influences the electron microscope phase contrast transfer function $\sin \chi(k)$, where k is the wave vector and

$$\chi(k) = \frac{2\pi}{\lambda}\left[-\frac{1}{4}C_s k^4 + \frac{1}{2}\Delta f k^2\right]$$

C_s is the spherical abberation constant and Δf the defocus value. In high-resolution imaging, one normally adjusts electron microscope defocus, Δf, so that the structure maxima coincide with the first minimum of the transfer function. The desired spatial frequencies can then be selected without any disturbing noise. However, in high-resolution imaging of beam-sensitive samples, the electron microscope has to be adjusted before exposing the sample to the beam, so that such a precisely defined defocus cannot normally be achieved. Inspection of Figure 2 shows that there is a weak second maximum in the $\sin^2 \chi(k)$ function near the second-order reflection from the smectic planes. However, because $\sin \chi(k)$ has passed through zero, this second reflection is transferred with contrast opposite to that of the first and would, in fact, adversely affect the

0024-9297/89/2222-0595$01.50/0

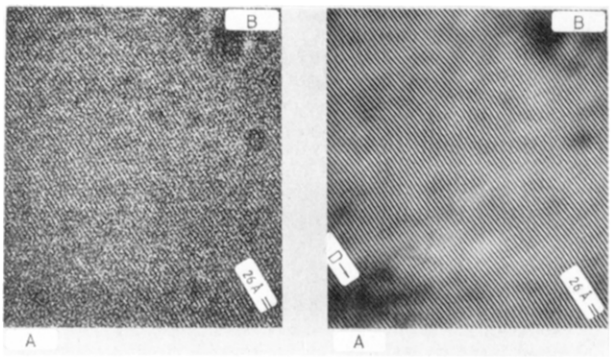

Figure 1. Electron micrograph and image reconstructed in light diffractometer: a, left; b, right.

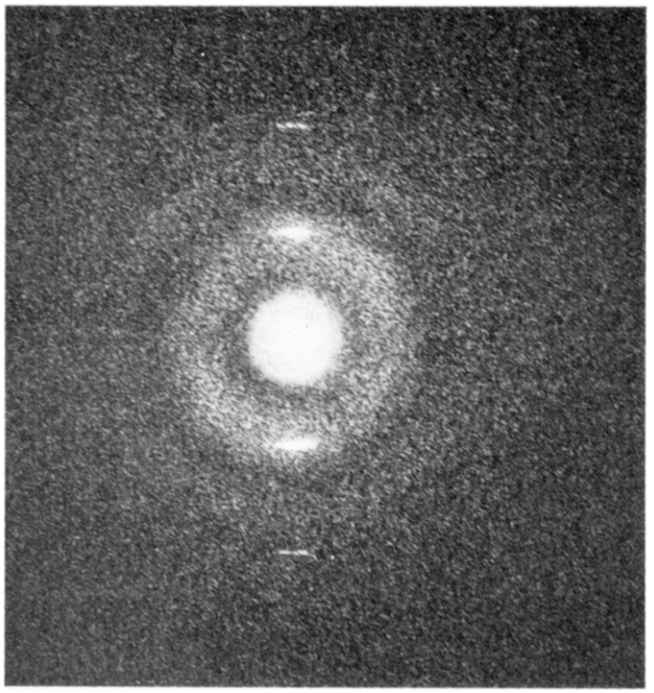

Figure 2. Light diffraction pattern obtained from electron micrograph showing smectic planes in a main-chain/side-group polymalonate.

image in the reconstruction process. If the phase of the second reflection could be reversed by π, both reflections could be used constructively to produce a better image. This latter step is, of course, only possible with digital methods. In principle, however, it should be easy to introduce a filter with apertures such that only the desired maxima in the diffraction pattern can contribute to the image formation.

This corresponds to the mathematical procedure of rejecting those spatial frequencies in the Fourier transform which are outside the chosen filter. In the experiment, however, good filtering is the crux of the whole operation and requires not only excellent optical components but perfect alignment of the filter apertures in the X, Y, and Z directions. It is well-known that spurious detail may appear in a computed electron density map if the terms included in the Fourier synthesis terminate too abruptly.[7,8] In the experiment, this is analogous to the effect of the aperture size. If the aperture is too small, we obtain the experimental equivalent of the spurious oscillations observed mathematically due to the integration cut-off effect. Experimentally the aperture has the same effect.

Figure 1 shows the undulating smectic planes in a main-chain/side-group polymalonate in the smectic state with a periodicity of 26 Å.[4] In our example of optical image

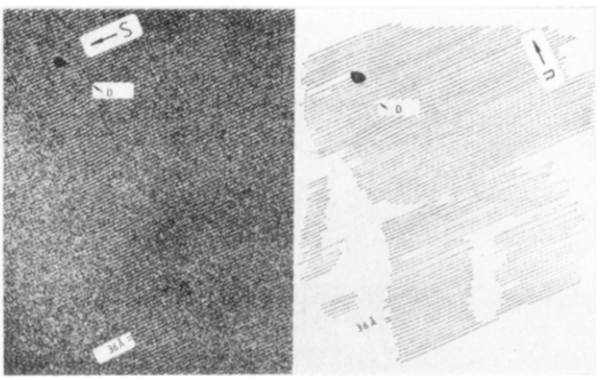

Figure 3. Electron micrograph and copy of transparent overlay showing edge dislocation D in smectic planes.

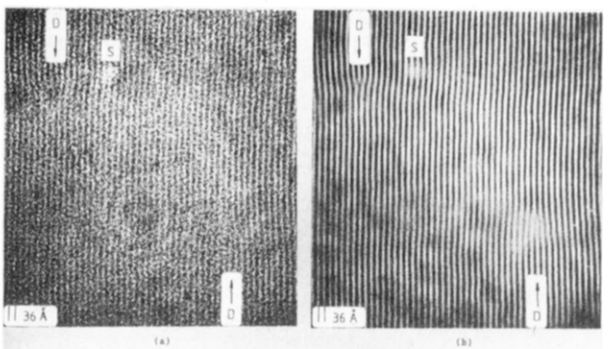

Figure 4. Original electron micrograph (a) and filtered image (b) showing dislocation.

reconstruction, the improvement in image quality is considerable. The dark region at B in the top right-hand corner of the electron micrograph and the diffractogram indicates that this is an identical region in the sample. The undulating nature of the smectic planes is well reproduced. An important observation in connection with this micrograph is the following: There is a region in the original micrograph at A in which the smectic planes are no longer visible. Due to the background noise, it is impossible to determine whether there is a preferred orientation in these regions or not. After the random noise is filtered, the results seem to indicate that there is continuation of the smectic planes in this region. Furthermore, a defect D appears (Figure 1b) which was not present in the original micrograph (Figure 1a). This important point will be taken up again in the Discussion section.

The next step in image reconstruction using a light diffractometer consisted in the analysis of dislocations which are present in the original micrograph. There is a problem here connected with the fact that phase information is lost in reciprocal space. Therefore in reconstruction, the information about the position of an aperiodic object is lost unless the phases are correctly recombined. Figure 3 shows a highly magnified electron micrograph of a main-chain polymolonate in the crystalline state with a copy of the transparent overlay. The periodicity of the lattice phases is 36 Å. It is not only very time consuming to produce a transparent overlay, it is also very difficult to avoid undue smoothing. Thus, for example, the lattice planes adjacent to the dislocation core at D curve much more smoothly in the overlay than is actually the case. The filtered image Figure 4b shows the true nature of these defects much more clearly. The original micrograph, Figure 4a, was chosen with a characteristic dirt spot at S in order to demonstrate that the position and nature of the dislocation are identical with the original micrograph, but the quality of the filtered image is in-

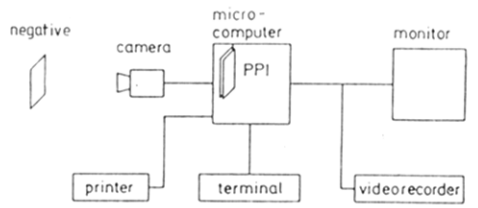

Figure 5. Schematic diagram showing hardware system for digital image analysis.

comparably better, showing the true nature of the dislocation core very clearly. Both dislocations are clearly visible in the original micrograph in the identical position. Thus, we have been able to avoid spurious effects. Furthermore, it has been possible to obtain a considerably improved image of the dislocation core using optical filtering. Disadvantages of the method are that optical filtering requires time-consuming alignment procedures and is not very versatile. For this reason, various computer techniques were applied and compared with the light diffractometer results.

Computer Simulation of Electron Microscope Images. (a) Off-Line Technique. Recently, the digital image processing technique has developed rapidly with the advance of computer science.[9,10] Image processing can be divided into three main sections: (1) image evaluation, (2) image handling, and (3) pattern recognition. In this section, an interactive picture analysis system (IAPA) used for image handling is described, and image enhancement is applied to some of the electron micrographs discussed above in order to improve the visual appearance of the images and to diminish the noise.

Device Description. The hardware system is shown in Figure 5 and described in detail elsewhere.[10] The image is recorded by a CCD camera and fed to the image processor of the computer. The digitized video signal is sent to the monitor or stored in the image storage device. The video camera (SONY XC-37) has a resolution of 384 × 491 elements. The microcomputer is a 16-bit microcomputer (Eltec E3) with 12-MHz frequency and 1-Mbyte memory capacity. The image processor has a memory capacity of 512 kbyte and converts the image to digital interlaced form in 40 ms. This enables two pictures to be stored with an 8-bit resolution of each pixel (corresponding to 256 gray levels).

Figure 6a shows a video picture of an electron microscope image recorded directly from the negative shown previously. The characteristic dirt spot S is again indicated. Registration is achieved by using a macrozoom camera objective so that the magnification of the image can be chosen freely. Some improvement of the visual appearance is achieved by two very simple operations using low- and high-pass filter techniques. With the low-pass technique, each picture element is sequentially examined. If the intensity of a picture element is greater or smaller than the average brightness of its immediate neighbors, it is replaced by the average value. Noise in an image generally has a higher spatial frequency spectrum than the normal image components because of its spatial decorrelation. Hence low-pass spatial filtering can also be effective for noise smoothing.

Improved contrast can be achieved by high-pass filtering, which accentuates edges. Application of these techniques is shown in Figure 6b. Another helpful operation is achieved by a two-dimensional discrete differentiation which can be performed by convoluting the original image array with compass gradient masks (i.e., north, east, south, west, northeast, etc.). The compass names indicate the

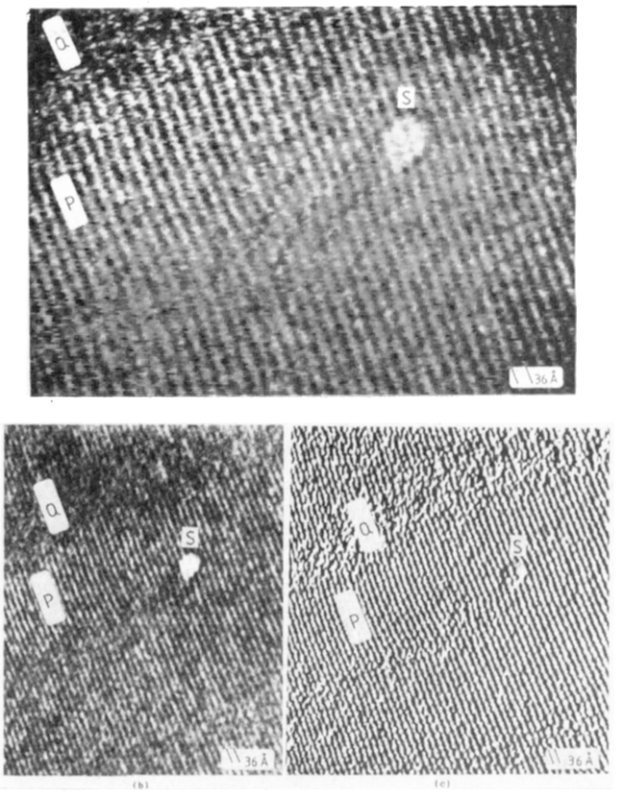

Figure 6. (a, top) Video picture of electron micrograph recorded directly from negative. (b, c) Video image of electron microscope negative using high- and low-pass filter techniques (b) and compass masks (c).

slope direction of maximum response; for example, the east gradient mask produces a maximum output for horizontal luminance changes from left to right. In Figure 6c, all these different compass masks are applied sequentially for image handling. It should be noted that parts b and c of Figure 6 have no more information than Figure 6a, but subjectively it is easier to recognize the form of the smectic planes. In all figures, the characteristic spot S is again indicated. However, it should be noted that an important feature must be investigated, namely, the apparently noncorrelated regions at Q in Figure 6a which indicate a preferred orientation after image processing (Figure 6c). In order to investigate this feature, the spatial correlation function was calculated for regions P and Q.[11]

The mathematical form of a spatial intensity autocorrelation function can be described by

$$R(\Delta x) = \lim_{N\to\infty} \frac{1}{N} \int_0^N \frac{I(x)\, I(x+\Delta x)}{\langle I^2 \rangle}$$

In the case of hypothetical "white noise" in which the intensities are distributed uniformly over the whole intensity range, the correlation function would be a Dirac δ function. Thus, the uncorrelated noise will not contribute to the correlation function. This operation was performed using an increment Δx of 1.8 Å, corresponding to one pixel at this magnification.

Figure 6b shows an electron micrograph with characteristic elongated regions showing clearly pronounced smectic planes at P. Between these regions at Q, there is considerable noise, so that it is not clear whether there is an orientation correlation or not. By calculation of the spatial correlation functions in these different regions, the situation becomes clear. The correlation function in region P (Figure 7, curve A) shows maxima and minima representing the periodicity of the periodic planes. The position

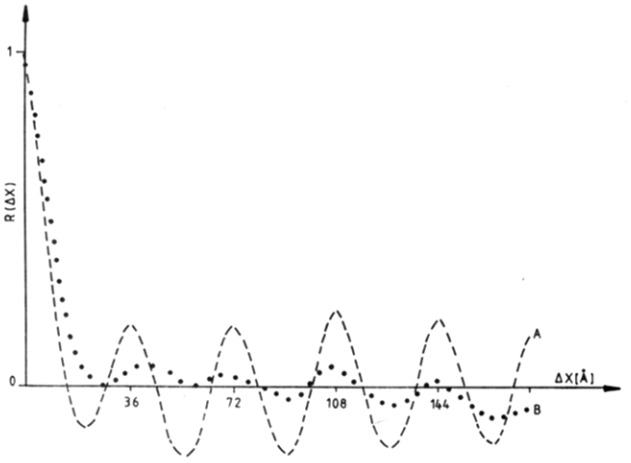

Figure 7. Spatial correlation function obtained from regions P and Q in Figure 6.

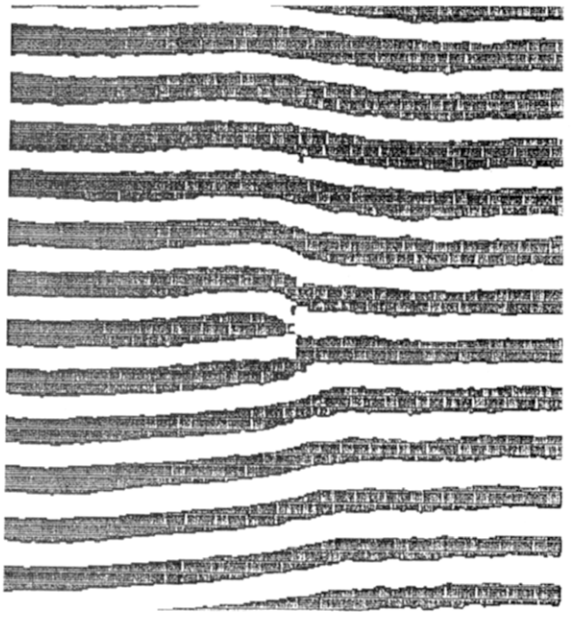

Figure 8. Enlarged representation of dislocation in Figure 6 using electronic zooming and clipping technique.

of the first maximum gives the distance between the planes. The correlation function from region Q (Figure 7, curve B) shows an identical periodicity, but the maxima and minima are not as well pronounced; i.e., the same correlations are clearly present in these regions. There are two possible explanations for this observation: (1) The order may not be as well developed in these regions. (2) The orientation of the smectic planes may not be exactly parallel to the electron beam.

In principle, this question could be solved by a series of tilting experiments, but in practice a high-resolution tilt series is impossible to perform with such beam-sensitive samples.

By use of the computer, a number of alternative representations of the smectic planes and dislocations can be chosen in order to highlight important details such as a dislocations (Figure 8). For this representation, the dislocation of Figure 4 was filtered by using a low-pass filter and enlarged by using electronic zooming. There are many alternative methods of representing such features, which are now available in standard software. The computer methods discussed so far involve filtering in real space. However, the micrograph can be digitized and its Fourier transform calculated.[12] Filtering can then be performed electronically in reciprocal space and a second Fourier

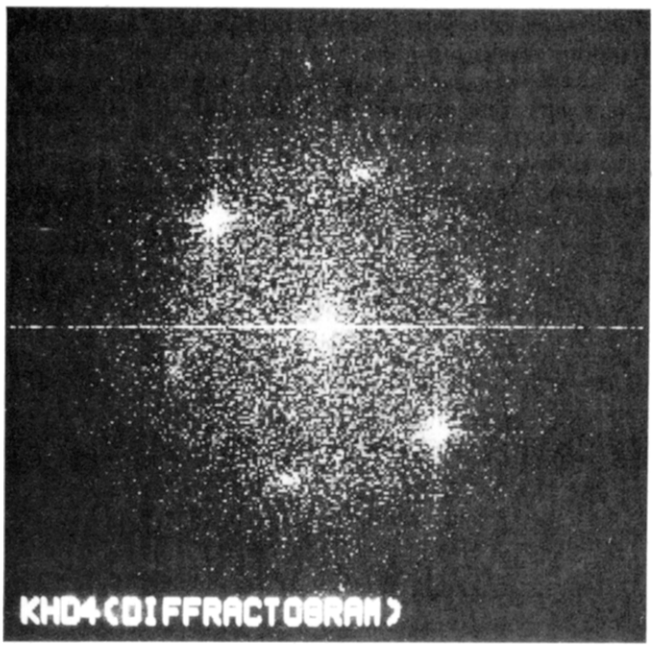

Figure 9. Computer diffractogram obtained by Fourier transformation of electron micrograph showing discotic liquid crystal.

transform calculated. This is the exact analogue of the optical diffractometry discussed earlier and also involves the same problems.

However, whichever technique or representation is chosen, the essential prerequisite is a good electron micrograph.

(b) On-Line Technique. A major advance is achieved by on-line image processing. As an example, we demonstrate this technique on a discotic main-chain liquid-crystal polymer. The disk-shaped molecules are stacked like a column of coins perpendicular to the film.[13] Imaging is performed at very low doses by using a video image intensifier system. In this case, correction of astigmatism, adjustment of defocus, and detection of drift are rapidly achieved by directly viewing the computer-calculated diffractogram of the electron image on a monitor (Figure 9). This is an enormous advantage in beam-sensitive samples. Filtering is performed electronically in reciprocal space and the filtered image reconstructed by Fourier transformation.

The system is a VME-Bus-based[14] multiprocessor system. The image obtained directly from the image intensifier is digitized and stored. The main processor is a 68010 Motorola CPU, and for the time-consuming algorithms of fast Fourier transformation, a special FFT processor board is used. The phases and amplitudes are stored, and the diffraction pattern of the image is displayed on a monitor (Figure 10). Continuous adjustment of defocus and astigmatism enables optimum contrast transfer to be achieved. The chosen frequencies for reconstruction are chosen electronically, and the information is fed to the computer. If necessary, desired phase changes can be accounted for. At the same time, the contrast transfer function for the electron microscope can be included by using appropriate software. The new filtered image is calculated by Fourier transformation. Another processor board together with two memory boards allows real-time addition and subtraction of video images. Radiation damage to the sample can be minimized by controlling the beam shutter of the electron microscope with the image processing system.

This powerful technique is demonstrated in Figure 11 for hexapentoxytriphenylene[14] viewed with the molecules

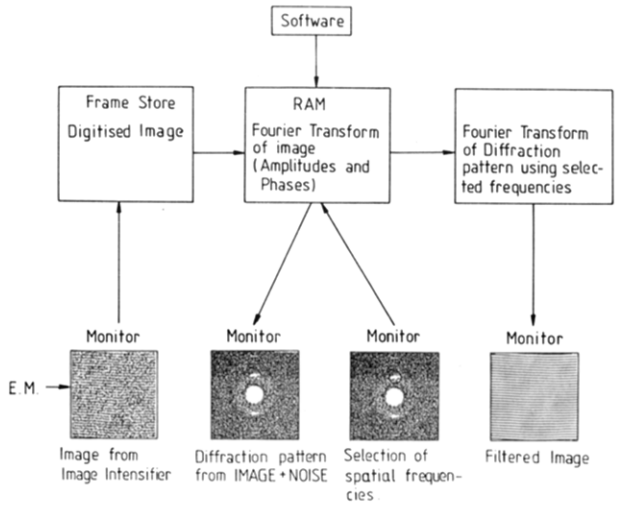

Figure 10. Schematic diagram showing on-line image analysis.

perpendicular to the film plane. Some of the columns are tilted, and a number of defects are visible in the original image (Figure 11a). These defects are enlarged and enhanced by image analysis (Figure 11b).

Discussion

A number of techniques for image analysis using light diffractometry and computer simulation techniques have been compared. They all involve filtering either in real or reciprocal space. Which technique is chosen is partly a financial question. In principle, all methods of image analysis contain the same inherent dangers.

Analysis in real space involves smoothing procedures which may delete real structure or overaccentuate nonstructural details. It is feasable that periodicity could be simulated. In our experience, the quality of the images is not very superior to that of the original micrograph. The real advantage lies in the enormous enlargement and therefore easier detection of defects. This is important in beam-sensitive samples because the original electron microscope magnification cannot be allowed to exceed 30000–50000. Dislocations are therefore extremely difficult to detect.

Reconstruction of the image via reciprocal space either off-line or on-line involves a number of difficulties which may cause spurious effects. We have demonstrated some of these by light diffractometry, and precisely the same difficulties arise in computer analysis. The diffraction pattern is the Fourier transform of the periodic lattice and consists of a set of δ functions. Only the Fourier frequencies containing this periodic information are normally selected by the aperture. In order to reconstruct the image, the Fourier transform of the δ functions is convoluted with the aperture function. The convolution effect leads to spatial averaging. This effect is well-known in mathematics[12] and beautifully illustrated in Taylor and Lipson's classical book (Plate 28).[7] The frequency of the spurious oscillations from the aperture is inversely proportional to the size of the aperture or, mathematically, to the integration limits.[8]

In principle, then, the aperture size or integration limit can be changed so that the size of the oscillations is far removed from the size of the structural details of interest. The problem arises as to how the aperiodic frequencies in reciprocal space caused by defects can be combined to account for phase changes on diffraction and correctly reproduce the position of aperiodic details such as dislocations. We have demonstrated this problem by light diffractometry in Figure 1, where a dislocation has clearly

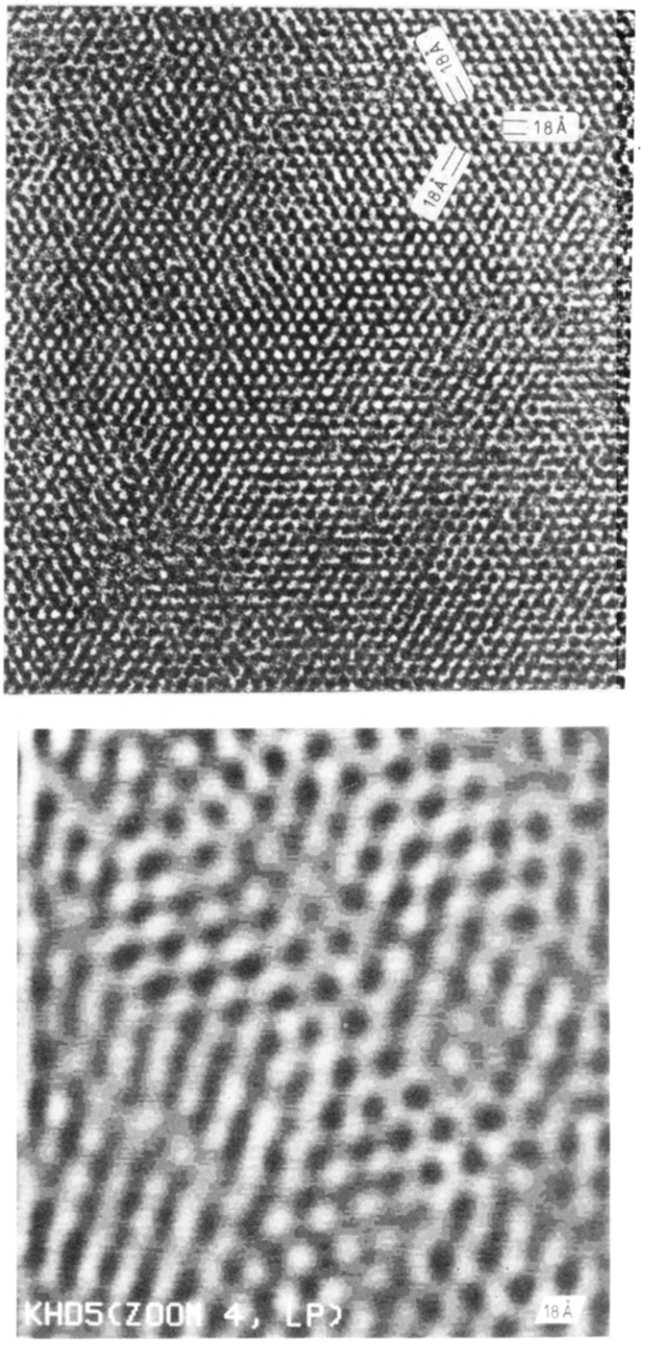

Figure 11. (a, top) Electron micrograph showing molecules in a discotic main-chain liquid crystal. (b, bottom) Image of discotic main-chain liquid crystal after computer filtering in reciprocal space.

appeared after reconstruction which was not in the original micrograph. However, other examples (Figure 4) show that correct reconstruction can be achieved. Precisely the same problem has been discussed for computer-calculated images in an excellent contribution[15] which was unfortunately published after this paper was submitted, so that a detailed comparative analysis of the two methods is no longer possible. These authors also point out that great care must be exercised in the interpretation of lattice defects. The problems in light diffractometry and digital analysis are identical. This is to be expected because the same physics is involved.

The aim now is to develop reliable and fast computer processing techniques for image reconstruction with the aid of these samples, because they have well-oriented structures with clearly defined defects which are visible

in the original micrographs[5] and can thus be compared with the reconstructed image.

Acknowledgment. This work has been supported by the Deutsche Forschungsgemeinschaft, Sonderforschungsbereich 262.

Registry No. Hexapentoxytriphenylene, 69079-52-3.

References and Notes

(1) Durst, H.; Voigt-Martin, I. G. *Makromol. Chem., Rapid Commun.* **1986**, *7*, 785.
(2) Voigt-Martin, I. G.; Durst, H. *Liq. Cryst.* **1987**, *2*(5), 585.
(3) Voigt-Martin, I. G.; Durst, H. *Liq. Cryst.* **1987**, *2*(5), 601.
(4) Voigt-Martin, I. G.; Durst; H.; Reck, B.; Ringsdorf, H. *Macromolecules* **1988**, *21*, 1620.
(5) Voigt-Martin, I. G.; Durst, H. *Macromolecules*, in press.
(6) Klug, A.; de Rosier, D. J. *Nature (London)* **1966**, *212*, 29.
(7) Taylor, C. A.; Lipson, H. *Optical Transforms*; Bell: London, 1964.
(8) Voigt-Martin, I. G.; Mijlhoff, F. C. *J. Appl. Phys.* **1976**, *47*, 3942.
(9) Pratt, N. K., Ed. *Digital Image Processing*; Wiley: New York, 1978.
(10) Wahl, F. M. *Digitale Bildsignalverarbeitung*; Springer-Verlag: Berlin, 1984.
(11) Krug, H.; Holoubek, J.; Fischer, E. W. *Colloid Polym. Sci.* **1987**, *265*, 779.
(12) Champeney, D. C. *Fourier Transforms and their Physical Applications*; Academic: New York, 1973; p 72.
(13) Voigt-Martin, I. G.; Brzezinski, V.; Durst, H.; Kreuder, W.; Ringsdorf, H., submitted for publication in *Nature (London)*.
(14) Tietz, R. *J. Microsc. Spectrosc. Electron.* **1986**, *11*, 65.
(15) Padere, P.; Revol, J. F.; Nguyen, L.; Manley, R. St. J. *Ultramicroscopy* **1988**, *25*, 69.

NMR Imaging of Elastomeric Materials

C. Chang and R. A. Komoroski*

Departments of Radiology, Pathology, and Biochemistry, University of Arkansas for Medical Sciences, Little Rock, Arkansas 72205. *Received March 3, 1988; Revised Manuscript Received June 28, 1988*

ABSTRACT: In order to establish the utility of NMR imaging for certain materials science applications, we have examined a number of elastomeric systems of similar glass transition temperature but differing chain segmental mobilities. As expected, the quality of the images is highly dependent on chain segmental mobility. Usable hydrogen images were obtained at ambient temperatures on two commercial imagers in reasonable times (one half-hour to overnight) for bulk *cis*-polybutadiene, natural rubber, and a cured, carbon-black-filled *cis*-polybutadiene. For typical 2D FT imaging where a spin echo is detected, image quality is, as expected, highly dependent on the relative values of T_2, the spin–spin relaxation time, and TE, the time to echo. Polyisobutylene, a rubber with the same T_g as natural rubber, but a $T_2 < 1$ ms, gave no image under the same conditions as for the other polymers. The polymers also were imaged by using a gradient–echo sequence. It appears that the gradient–echo sequence, which is sensitive to T_2^*, may be better than the spin–echo sequence, which is sensitive to T_2, for detection of defects such as voids, gaps, or small foreign particles in elastomers. This results from a magnification effect caused by magnetic susceptibility differences at the void surface. A crude resolution test was performed by using the spin–echo sequence on multiple sheets of cured, filled *cis*-polybutadiene separated by NMR-transparent spacers of variable width. Features as small as 0.07 mm could be detected even though the pixel size was 0.47 mm.

Introduction

Nuclear magnetic resonance imaging has evolved into an important diagnostic modality in clinical medicine over the last 10 years.[1,2] Although the technique can be performed in a number of ways, in every case it provides a picture of NMR signal intensity as a function of location (in one, two, or three dimensions) in an object. Depending on technique details, the location-dependent NMR signal is a function of local spin concentration and local spin–lattice (T_1) and spin–spin (T_2) relaxation times. As for typical high-resolution NMR spectroscopy, NMR imaging detects only the liquid or liquidlike components in the human body—mainly water and fat.

Whereas the clinical applications of NMR imaging have developed quite rapidly, applications in materials and polymer science have been slow to appear. This is due in part to the fact that commercial NMR imaging equipment suitable for such studies has become available only recently. It also arises from the more or less well founded belief that most important applications in materials science involve rigid solids, which cannot be studied by using standard equipment. Nevertheless, a number of nonmedical applications of NMR imaging has appeared. The majority of these reports deals with diffusion of liquids through rock,[3-11] wood,[12-15] or polymers.[16-19] Suits and White have imaged ionic distribution[20] and temperature profile[21] in solid ionic substances.

Efforts are currently underway on the development of NMR imaging techniques for rigid solids.[20-33] Solids pose formidable problems for standard NMR imaging techniques. The spread of frequencies imposed by the gradient forming the image must be larger than the linewidth. Typical solid-state proton line widths are on the order of 20 kHz, a value that precludes NMR imaging of rigid solids using standard gradient strengths of about 1–2 G/cm. Among the approaches being tried for rigid solids are line narrowing by multiple-pulse,[28,32] rotating-frame magic-angle,[30] laboratory-frame magic angle,[33] solid echo,[31] and heteronuclear-decoupling[25] techniques, multiple-quantum NMR to magnify the effect of the field gradient,[24,26] combined multiple-pulse sequences and radio-frequency (rf) field gradients,[29] and incrementing the field gradient during a fixed evolution time.[27] In addition, instrument manufacturers are beginning to provide systems with more powerful gradients, from 20 to 200 G/cm or greater.[34,35] For the most part these systems are geared to obtaining high-resolution NMR images of small but not necessarily rigid objects. Additional development work is necessary before the above and related techniques see widespread use for imaging truly rigid solids in materials or polymer

0024-9297/89/2222-0600$01.50/0